

## EFFECT OF CALCITE SCALING ON PRESSURE TRANSIENT ANALYSIS OF GEOTHERMAL WELLS

Serkan Arkan, Serhat Akin, Mahmut Parlaktuna

Middle East Technical University  
Department of Petroleum and Natural Gas Engineering  
06531 Ankara-TURKEY  
e-mail: serhat@metu.edu.tr

### ABSTRACT

Build-up measurements from five wells (KD-6, KD-15, KD-16, KD-21, and KD-22) of Kizildere Geothermal field were analyzed. The main focus was to investigate the effect of calcite scaling on reservoir and wellbore parameters such as permeability, skin factor, wellbore storage coefficient. Several buildup tests from the same well before and after cleaning operations were interpreted to achieve this goal. The analyses of data showed that, it is possible to quantify the effect of calcite scaling on reservoir and wellbore parameters. It was also observed that some of the buildup tests were run at two-phase conditions and the results from these tests are erroneous

### KIZILDERE GEOTHERMAL FIELD

The Kizildere geothermal field was discovered in 1968. It is located in the Denizli and Aydin provinces of western Turkey (Figure 1) at the Western extreme of the Büyük Menderes graben (Figure 2). The Menderes massif was uplifted during late Pliocene and Quaternary times, and east-west grabens formed as a result of tensional forces. Magma rose under the massif and under the grabens where the earth's crust is thinner. Thus, the geothermal fields occur naturally along the grabens and the Kizildere field is an example (Simsek, 1985). The field lies on three main fault blocks, generated by two-step normal faults, running nearly parallel to the flank of the Menderes Valley. The area is rich with geothermal manifestations, including water springs at a temperature between 30 °C and 100 °C.

Kizildere geothermal field in the exploited region consists of two producing reservoirs in the intermediate block within the depths explored. The main reservoir, Igdecik formation, is sited in the metamorphic basement, and composed of crystalline limestones, which has high fracture permeability. Sazak, a limestone formation, is the minor producing zone and lies above Igdecik. Kizilburun, Kolonkaya formations and locally Sazak formation form the caprock. The maximum temperatures of Sazak and

Igdecik formations are 198 °C and 209.1 °C, respectively.

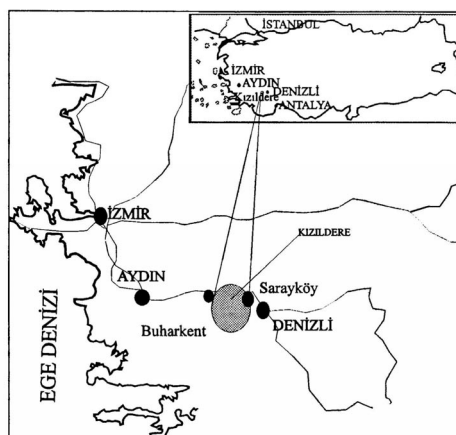


Figure 1. Location of Kizildere Geothermal Field (Aksoy, 1997).

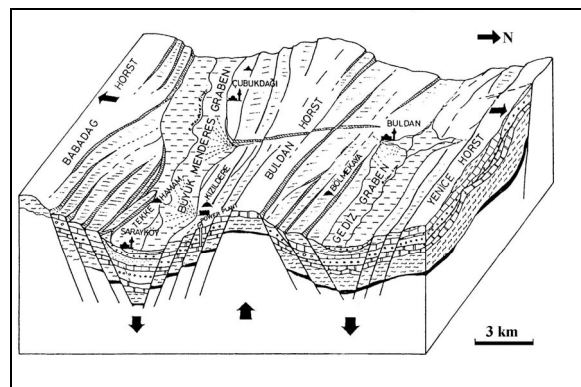


Figure 2. Horst-Graben Systems in Western Anatolia (Simsek, 1985).

The first well, KD-1, drilled in 1968 to a depth of 540 m, produced a mixture of water and steam with a temperature of 198 °C in the reservoir, thus indicating the existence of a water-dominated geothermal system. Later, 17 wells more have been drilled in this field. A geothermal power plant with a capacity of 20.4 MWe was put in operation in 1984. Three additional production wells were drilled in

1986 due to the shortage of steam. The depths of the wells are between 370 m-1241 m.

Kizildere geothermal field has three main problems: Calcite scaling in the production wells and surface connections, depletion of reservoir pressure due to production, and the disposal of wastewater with high boron content (25-30 ppm) into B.Menderes River.

### **Calcite scaling in the production wells and surface connections:**

Geothermal fluid at Kizildere Geothermal field contains high  $\text{CaCO}_3$  and 1-1.5 % dissolved  $\text{CO}_2$  by weight (Simsek, 1985). The  $\text{CO}_2$  partial pressure drop that takes place during the flow of geothermal fluid causes calcite scaling. Calcite scale causes a reduction in well bore radius thus a decrease in productivity of the well bore. Because of the higher costs of scale inhibitor injection and acidizing, mechanical reaming appeared as the most economical method with Rotating Control Head Preventer (RCHP) to remove calcite of the wells. Figure 3 shows daily production rates between 1989 and 2000. The production rate reaches its maximum right after cleaning work, but it starts to decline immediately after a short production period due to calcite scaling. These effects are also felt in pressure decline curves as peaks right after cleaning (Fig. 4).

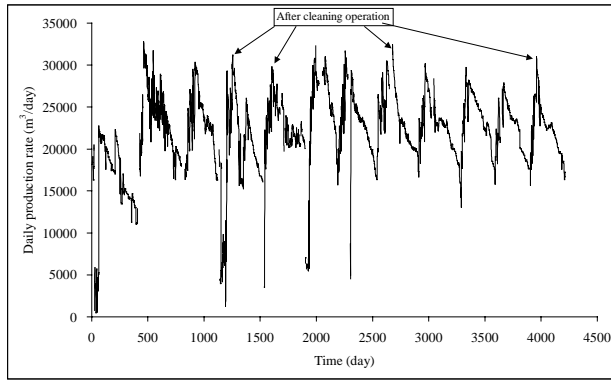


Figure 3. Daily production rate of Kizildere geothermal field (Yeltekin, 2001).

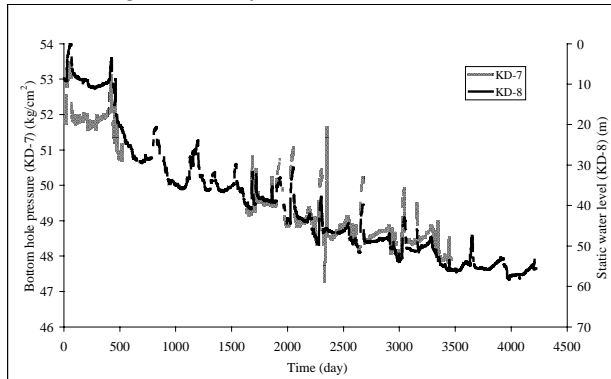


Figure 4. Pressure decline in observation wells (1988-2000) (Yeltekin, 2001).

In this study, effects of calcite scaling on the pressure transient analysis of several drawdown tests, conducted before and after mechanical reaming are presented. The drawdown data is analyzed by different well test analysis models. The changes in skin, permeability thickness product, storativity and conductivity ratios are analyzed. It was observed that the results change significantly.

## **THEORY**

### **Pressure Transient Tests**

Geothermal wells generally produce from fractured volcanic rocks. As reported by Barenblatt et al (1960), a porous rock with a highly developed system of fissures can be represented as the superposition of two porous media with pores of different sizes. Warren and Root (1963) presented a model based on above mathematical concept of superposition. They idealized a naturally fractured reservoir such that the material with the primary porosity is contained within a systematic array of identical rectangular parallelepipeds. The secondary porosity is contained within an orthogonal system of continuous uniform fractures which are oriented parallel to one of the principal axes of permeability. In this model, the dual porosity effects are described in terms of two parameters that relate primary and secondary properties. The first of the two parameters is the storativity ratio,  $\omega$  that relates the fracture storativity to that of the combined flow:

$$\omega = \frac{\phi_f C_{tf}}{\phi_f C_{tf} + \phi_m C_{tm}} \quad (1)$$

Values of  $\omega$  can be less than or equal to one. The case of  $\omega = 1$  occurs if the matrix porosity is zero, hence it implies that the reservoir is a single porosity one (Horne 1995). The second parameter is dependent on the transmissivity ratio, and is designated as  $\lambda$ :

$$\lambda = \alpha \frac{k_m}{k_f} r_w^2 \quad (2)$$

Here  $\alpha$  is a factor that depends on the geometry of the interporosity flow between the matrix and the fractures:

$$\alpha = \frac{A}{xV} \quad (3)$$

where  $A$  is the surface area of the matrix block,  $V$  is the matrix volume, and  $x$  is a characteristic length. If the matrix blocks are cubes or spheres, then the interporosity flow is three dimensional and  $\lambda$  is given by

$$\lambda = \frac{60k_m}{x_m^2 k_f} r_w^2 \quad (4)$$

Here  $x_m$  is the length of a side of the cubic block, or the diameter of the spherical block. If the matrix blocks are long cylinders, then the interporosity flow is two dimensional and  $\lambda$  is given by

$$\lambda = \frac{32k_m}{x_m^2 k_f} r_w^2 \quad (5)$$

where  $x_m$  is now the diameter of the cylindrical block. If the matrix blocks are slabs overlying each other with fractures in between, then the interporosity flow is one dimensional, and  $\lambda$  is given by

$$\lambda = \frac{12k_m}{h_f^2 k_f} r_w^2 \quad (6)$$

Here  $h_f$  is the height of the secondary porosity slab. Values of  $\lambda$  are usually very small (usually,  $10^{-3}$  to  $10^{-10}$ ). If the value of  $\lambda$  is larger than  $10^{-3}$ , the level of heterogeneity is insufficient for dual porosity effects to be of importance, and again the reservoir acts as a single porosity (Horne 1995) as in the case of  $\omega = 1$ . Analysis of pressure transient tests is usually conducted by combining type-curve matching and semi-logarithmic techniques in a computer-aided manner (Horne, 1995).

## RESULTS AND DISCUSSIONS

Several different wells for the analysis of scaling effects on pressure transient response of the wells were selected. The selection was partially based on the availability of data and the down-hole conditions. Thus, wells that have steam at bottom hole conditions were selected by checking the saturation pressure obtained by Equation. 7.

$$P_{Saturation} = P_{CO_2} + P_{Steam} \quad (7)$$

$$P_{CO_2} = \frac{n_1}{\alpha(T)} \quad (8)$$

where  $n_1$  is the weight per cent of  $CO_2$  in liquid phase ( $n_1 = 0.0142$  at  $200^\circ C$  in Kizildere) and  $\alpha(T)$  can be calculated from Sutton (1976) equation given below.

$$\alpha(T) = \left[ 5.4 - 3.5 * \left( \frac{T}{100} \right) + 1.2 * \left( \frac{T}{100} \right)^2 \right] * E^{-9} \quad (9)$$

Thus for each well the saturation pressure was estimated for different temperatures using Table 1. It was observed that only two wells were producing with single phase: KD-6 and KD-21. After preliminary selection three more wells KD-15, KD-16, and KD-22 (Fig. 5) were also used for modeling and comparing the scale effects.

Table 1. Saturation pressures

T (°C)	P <sub>CO2</sub> (bars)	P <sub>steam</sub> (bars)	P <sub>saturation</sub> (bars)
150	49.82	4.76	54.58
160	49.44	6.18	55.62
170	48.66	7.92	56.58
180	47.52	10.03	57.55
190	46.07	12.55	58.62
200	44.38	15.55	59.93
210	42.49	19.08	61.57

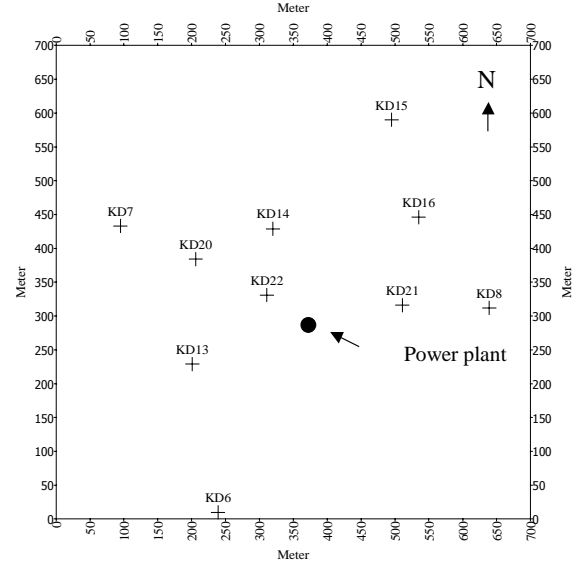


Figure 5. Locations of wells used in pressure transient analysis.

Analyses of pressure transient tests were carried out in a systematic manner. The first step consisted of conventional semilog and type curve analysis (Horne 1995). Initial parameter estimates for several reservoir parameters like permeability were obtained at this stage. Then these estimates were fine tuned using an automated history matching technique. The estimated parameters were accepted using 10% confidence intervals. The analyses were conducted using a commercial well test analysis package named Saphir (Kappa, 2001). During the estimation procedure three types of wellbore conditions were considered: wellbore storage and skin, finite conductivity vertical fracture, and infinite conductivity vertical fracture. The models and their different combinations presented in Table 2 were used to match drawdown data before and after mechanical reaming. Homogeneous storage and skin model is one of the most generally used well test models to represent geothermal reservoir conditions. Large wellbore storage coefficient is common in geothermal wells due to the large wellbore volume and the compressibility of the steam-water mixture in the wellbore. Large, negative skin values calculated are consistent with the theory that since geothermal

wells generally produce from fractured volcanic rocks they show stimulated behavior (Horne 1995).

It has been observed that, for most cases since the boundary effects were visible the use of “Closed Circle” and “Closed Rectangle” boundary conditions was necessary. Hence, “Infinite Acting” boundary condition was not used for the analyses. Similarly, both transient and pseudo steady state double porosity model results were close to each other leaving only three possible and equally probable models: 1) storage-skin homogeneous model, 2) finite conductivity fracture wellbore with transient double porosity model and 3) storage-skin homogeneous infinite acting model. The results obtained using different models are demonstrated by analyzing data from well KD-6.

Table 2. Different Well Test Models Used for the Analysis

Model	1	2	3
Wellbore	Storage Skin	Finite Conductivity Fracture	Storage Skin
Reservoir	Homogeneous	Dual Porosity Transient	Dual Porosity Transient
Boundary	Infinite Acting	Closed Circle	Closed Circle

At the well temperature of 190°C the saturation pressure is 58.62 bars (Table 1). The minimum pressure at KD-6 is 59.709 bars that corresponds to single phase conditions. The analysis results are summarized in Figure 6 and tabulated in Table 3. It could be seen that infinite acting radial flow period has not been reached. The systems pressure derivative response shows a constant pressure closed boundary effect. The results are consistent with typical responses of a double porosity geothermal system such that  $\omega$  and  $\lambda$  are small and the storage and permeability thickness product is somewhat high. The pressure transient data for other wells showed a similar behavior as well. Thus, in the analyses a double porosity, storage-skin, closed circle boundary model was used.

The same analysis procedure was applied to drawdown data obtained from some wells in Kizildere (KD-6, KD-15, KD-16, KD-21, and KD-22). The results of the analyses are given in Tables 4 through 8, respectively. In all these tables the columns were organized in such a way that different dates after mechanical reaming (DAMR) are investigated.

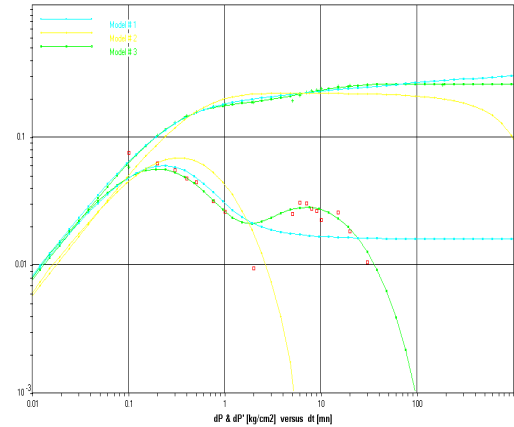


Figure 6. Comparison of three models for KD-6 drawdown data obtained 97 DAMR.

Table 3. Results for KD-6, 97 days after mechanical reaming (DAMR)

Parameter\ Model	1	2	3
Storage ( $m^3 cm^2/kg$ )	295	288	310
Skin	-3.27	0	-8.42
$k$ (md)	264	232	38.9
$kh$ (md.m)	27200	23900	4010
$\omega$	-	0.015	0.0615
$\lambda$	-	8.88E-6	3.26E-8

Large, negative skins were observed in most wells (Figure 7). In all the analyses the skin value increased as DAMR increased except for wells KD-6, KD-15, and KD-16. The reason for this behavior could be related to the fact that the rate of scaling is a second order polynomial function of flow rate (Satman et al., 1999). Since KD-16 is the highest producing well (168 tons/hr) and it has a larger diameter at the production interval it is possible that the scaling was more compared to the rest of the wells. Likewise, KD-15 is the second largest producing well (131 tons/hr) subject to large scaling that supports the above discussion. KD-6 on the other hand, has large  $CO_2$  content, 15% by weight, which makes it subject to higher scaling. Numerical quantification of skin factor as a linear or nonlinear function of DAMR was not possible.

Table 4. Results for KD-6 for Different Dates

Parameter\DAMR	97	143
Skin	-8.42	-11.1
$k$ (md)	38.9	4.28
$kh$ (md.m)	4010	441
$\omega$	0.0615	0.000448
$\lambda$	3.26E-8	1.56E-8

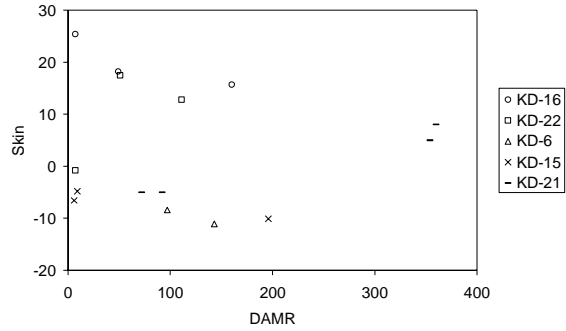


Figure 7. Change in skin factor for different wells as a function of DAMR.

Permeability and permeability-thickness products were quite high revealing the fractured nature of the reservoir. In general, the permeability decreased drastically as DAMR increased with a few exceptions (Figure 8). This can be explained by the fact that the scaling rate is proportional to  $q^2/k$  (Satman et al., 1999). The general trend was more pronounced in wells where the  $CO_2$  content was higher (i.e. KD-6).

Table 5. Results for KD-15 for Different Dates

Parameter\ DAMR	6	196	9
<i>Skin</i>	-6.57	-10.1	-4.83
<i>k (md)</i>	126	4260	234
<i>kh (md.m)</i>	3920	132000	7254
$\omega$	0.0969	0.14	0.16
$\lambda$	7.5E-7	0.00206	6.34E-5

Table 6. Results for KD-16 for Different Dates

Parameter\ DAMR	49	7	160
<i>Skin</i>	18.2	25.4	15.7
<i>k (md)</i>	361	376	91.4
<i>kh (md.m)</i>	47800	52600	13000
$\omega$	0.0999	0.00209	5.61E-7
$\lambda$	2.8E-6	8.17E-7	9.54E-13

Table 7. Results for KD-22 for Different Dates

Parameter\ DAMR	51	111	7
<i>Skin</i>	17.5	12.8	-0.8
<i>k (md)</i>	1030	400	19.5
<i>Kh (md.m)</i>	90000	34800	1700
$\omega$	0.1	0.0432	1.2E-1
$\lambda$	2.82E-6	1.5E-8	9.3E-6

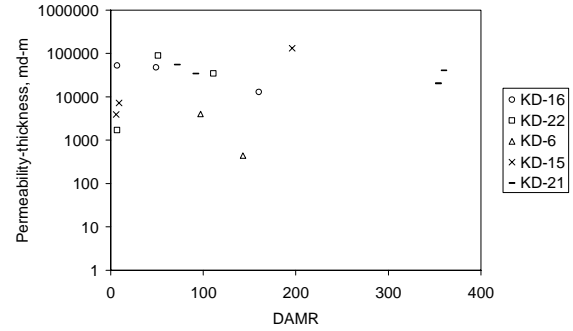


Figure 8. Change in permeability-thickness product for different wells as a function of DAMR.

Storativity ratios were somewhat scattered and less than 0.1 (Figure 9) for all wells. The storativity ratio values did not change as DAMR increased. Since storativity ratio is not a parameter that is expected to change the results can be considered normal. On the other hand, the transmissivity ratios showed a decreasing trend as DAMR increased (Figure 10). Since transmissivity ratio is the ratio of matrix to fracture permeability, this implies that the plugging due to calcite scaling is more pronounced in the matrix than the fractures for matrix-fracture situation. For a completely fractured system in which some of the fractures are acting like rock matrix, this implies that wide fractures providing the main flow are not plugged.

The aforementioned discussions and conclusions were reached based on the assumption that the analysis results were unique. However, it is quite possible that due to insufficient data sampling the matches may not represent the true system response. In such a case the results may not be accepted as general conclusions.

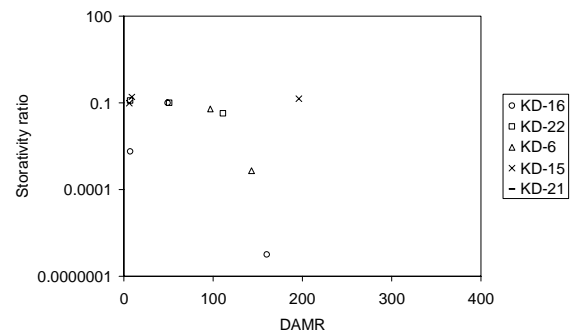


Figure 9. Change in storativity ratio for different wells as a function of DAMR.

Table 8. Results for KD-21 for Different Dates

Parameter\ DAMR	360	72	354	92
<i>Skin</i>	8.01	-5	4.97	-5
<i>k (md)</i>	127	173	63.8	100
<i>kh (md.m)</i>	40800	55300	20400	34500

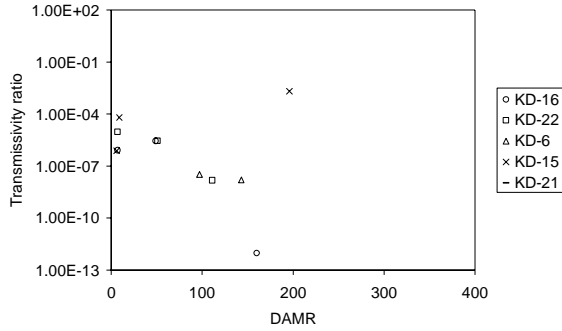


Figure 10. Change in transmissivity ratio for different wells as a function of DAMR.

## CONCLUSIONS

Analyses of geothermal well tests before and after mechanical reaming for the removal of calcite scaling are presented. Based on the results it was concluded that skin factor, permeability, permeability-thickness product, and transmissivity ratio decreased after mechanical reaming. Calcite deposition was more pronounced in wells where the production and CO<sub>2</sub> content was relatively high. Calcite deposition may affect the transient pressure response of the wells resulting in non-unique analysis.

## NOMENCLATURE

A	= area, m <sup>2</sup>
DAMR	= days after mechanical reaming, days
C <sub>tf</sub>	= fracture compressibility, bar <sup>-1</sup>
C <sub>tm</sub>	= matrix compressibility, bar <sup>-1</sup>
h	= thickness, m
k <sub>f</sub>	= fracture permeability, bar <sup>-1</sup>
k <sub>m</sub>	= matrix permeability, md
n <sub>l</sub>	= concentration of CO <sub>2</sub> in liquid phase (wt%)
r <sub>w</sub>	= wellbore radius, m
p	= pressure, bars
T	= temperature, °C
V	= matrix volume, m <sup>3</sup>
x	= length, m
α	= geometric factor
α(T)	= temperature function in Sutton equation
λ	= transmissivity ratio, dimensionless
φ <sub>f</sub>	= fracture porosity, dimensionless
φ <sub>m</sub>	= matrix porosity, dimensionless
ω	= storativity ratio, dimensionless

## REFERENCES

- Aksoy, N., (1997) "Kızıldere (Denizli) Jeotermal Enerji Sahasının Reenjeksiyon Olanakları" M.Sc. Thesis, Dokuz Eylül University (in Turkish).
- Barrenblatt, G.I., Zheltov, I.P. and Kochina, I.N., (1960), 'Basic concepts in the Theory of Homogeneous Liquids in Fissured Rocks,' J. Appl. Math. Mech., no. 24, 1286-1303.
- Horne, R.N., (1995), "Modern Well Test Analysis-A Computer Aided Approach," Petroway Inc., Palo Alto, CA, U.S.A.
- KAPPA Engineering, (2001), "SAPHIR V2.30 T Well Interpretation Package"
- Satman A., Ugur Z., and Onur M., (1999), "The Effect of Calcite Deposition on Geothermal Well Inflow Performance," Geothermics, 28, 425-444.
- Simsek, S., (1985) "Geothermal Model of Denizli, Sarayköy-Buldan Area" Geothermics, 14 , No.2/3 , 393-417.
- Sutton, F.M., (1976) "Pressure-Temperature Curves for a Two-Phase Mixture of Water and Carbon Dioxide", New Zealand Journal of Science, vol. 19, 297.
- Warren, J.E. and Root, P.J., (1963), "The Behaviour of Naturally Fractured Reservoirs," SPE Journal, September, 245-255.
- Yeltekin K., (2001), "Characterization and Modelling of Kizildere Geothermal Field" Msc thesis, Middle East Technical University, Ankara, Turkey.